Infrared spectroscopic study of hydrogen bonding topologies in the water octamer: The smallest ice cube

Gang Li
Dalian Institute of Chemical Physics
Yang-Yang Zhang
Tsinghua University
Qinming Li
State Key Laboratory of Molecular Reaction Dynamics, Dalian Institute of Chemical Physics, Chinese Academy of Sciences
Chong Wang
Dalian Institute of Chemical Physics
Yong Yu
State Key Laboratory of Molecular Reaction Dynamics, Dalian Institute of Chemical Physics, Chinese Academy of Sciences
Bingbing Zhang
Dalian Institute of Chemical Physics
Hanshi Hu
Tsinghua University
Weiqing Zhang
Dalian Institute of Chemical Physics
Dongxu Dai
Dalian Institute of Chemical Physics
Guorong Wu
Dalian Institute of Chemical Physics, Chinese Academy of Sciences. https://orcid.org/0000-0002-0212-183X
Donghui Zhang
Dalian Institute of Chemical Physics, Chinese Academy of Sciences https://orcid.org/0000-0001-9426-8822
Ling Jiang
Dalian Institute of Chemical Physics
Jun Li
Tsinghua University
Xueming Yang (xmyang@dicp.ac.cn)

Dalian Institute of Chemical Physics https://orcid.org/0000-0001-6684-9187

Article

Keywords: water octamer, hydrogen bonding topology, sharp vibrational bands features, hydrogen-bonding network

Posted Date: August 12th, 2020

DOI: https://doi.org/10.21203/rs.3.rs-53182/v1

Version of Record: A version of this preprint was published at Nature Communications on October 28th, 2020. See the published version at https://doi.org/10.1038/s41467-020-19226-6.

Infrared spectroscopic study of hydrogen bonding topologies in the water octamer: The smallest ice cube

Gang Li[1]*, Yang-Yang Zhang[2]*, Qinming Li[1,3]*, Chong Wang[1,3], Yong Yu[1,3], Bingbing Zhang[1], Han-Shi Hu[2], Weiqing Zhang[1], Dongxu Dai[1], Guorong Wu[1], Dong H. Zhang[1], Ling Jiang[1]†, Jun Li[2,4]†, Xueming Yang[1,4]†

[1]State Key Laboratory of Molecular Reaction Dynamics, Dalian Institute of Chemical Physics, Chinese Academy of Sciences, Dalian 116023, China.

[2]Key Laboratory of Organic Optoelectronics & Molecular Engineering of the Ministry of Education, Department of Chemistry, Tsinghua University, Beijing 100084, China.

[3]University of Chinese Academy of Sciences, 19A Yuquan Road, Beijing 100049, China.

[4]Department of Chemistry, Southern University of Science and Technology, Shenzhen 518055, China.

*These authors contributed equally to this work.

†Corresponding author. E-mail: xmyang@dicp.ac.cn (X.Y.); ljiang@dicp.ac.cn (L.J.); junli@tsinghua.edu.cn (J.L.).

Abstract

The water octamer, with its cubic structure consisting of six four-membered rings, presents an excellent system in which to unravel the cooperative interactions driven by subtle changes in the hydrogen-bonding topology. Although many distinct structures are calculated to exist, it has not been possible to extract the structural information encoded in their vibrational spectra because this requires size-selectivity of the neutral clusters with sufficient resolution to identify the contributions of the different isomeric forms. Here we report the size-specific infrared spectra of the isolated cold, neutral water octamer using a scheme based on threshold photoionization using a tunable vacuum ultraviolet free electron laser. A plethora of sharp vibrational bands features are observed for the first time. Theoretical analysis of these patterns reveals the coexistence of five cubic isomers, including two with chirality. The relative energies of these structures are found to reflect topology-dependent, delocalized multi-center hydrogen-bonding interactions. These results demonstrate that even with a common structural motif, the degree of cooperativity among the hydrogen-bonding network creates a hierarchy of distinct species. The implications of these results on possible metastable forms of ice are considered.

As the most vital matter on the earth, water and its interactions with other substances are essential in the life of our planet. Understanding the structure of bulk water and its hydrogen-bonding networks, however, remains a grand challenge[1,2]. Spectroscopic investigation of water clusters provides a quantitative description of hydrogen-bond motions that occur in ice and liquid water[3,4]. Currently, cationic or anionic forms of water clusters have been extensively investigated because of relative ease in size-selection and detection[5-9]. These studies have provided essential knowledge on the structure and dynamics of the ionic water clusters.

Inasmuch as hydrogen-bonding networks in neutral water clusters are substantially different from those in ionic ones, to investigate neutral water clusters is a prerequisite to gain fundamental insights into the structures and properties of ice and liquid water. Previous experimental and theoretical studies demonstrated that the water trimer, tetramer, and pentamer all have cyclic minimum-energy structures with all oxygen atoms in a two-dimensional plane, while the hexamer and heptamer have rather complex three-dimensional noncyclic structures[10-18]. Of particular interest is the water octamer, which was proposed to represent the transition to cubic structures dominated in larger systems and display behavior characteristic of a solid ↔ liquid phase transition[19-22]. Experiments strongly suggest the presence of ice nanocrystals[23-26]. The hydrogen bonds within the mostly crystalline subsurface layer are found to be stretched by the interaction with the diverse component[25]. The water octamer has thus become a superb benchmark for accurate quantification of the hydrogen-bonding interactions that govern the surface and bulk properties of ice.

Experimental characterization of the water octamer has been awkward due to the difficulty in size-selection and detection of neutral water clusters in general. Only a few gas-phase studies have been achieved[27-30], and two nearly isoenergetic structures with D_{2d} and S_4 symmetry are found. Here we report the well-resolved infrared (IR) spectra of confinement-free, neutral water octamer based on threshold photoionization using a tunable vacuum ultraviolet free electron laser (VUV-FEL). Distinct new features observed in the spectra identify additional cubic isomers with C_2 and C_i symmetry, which coexist with the global-minimum D_{2d} and S_4 isomers at finite temperature of the experiment. Analysis of the electronic structure reveals a remarkable stability of these cubic water octamers arising from extensively

delocalized multi-center hydrogen-bonding interaction. Multiple coexisting cubic octamers provide a coherent picture of structural diversity of bulk water and a cluster-scale precursor to the phase transition between solid and liquid water.

The vibrational spectra were obtained using a VUV-FEL-based IR spectroscopy apparatus described in detail in the supplementary information (SI)[31]. In the experiment, neutral water clusters were generated by supersonic expansions of water vapor seeded in helium using a high-pressure pulsed valve (Even-Lavie valve, EL-7-2011-HT-HRR) that is capable of producing very cold molecular beam conditions[32]. For the IR excitation of neutral water clusters, we used a tunable IR optical parametric oscillator/optical parametric amplifier system (LaserVision). Subsequent photoionization was carried out with about 30 ns delay with a VUV-FEL light at 113.30 nm delivered by the Dalian Coherent Light Source (DCLS) facility. IR spectra were recorded in the difference mode of operation (IR laser on−IR laser off).

The experimental IR spectrum of $(H_2O)_8$ in the OH stretching region is shown in the bottom of Fig. 1 and the band positions are listed in Table S1. The comparison of present and previously measured spectra is given in Fig. S1. From Fig. S1, the present spectrum displays three distinct new absorptions at 2980, 3002, and 3378 cm^{-1}; the 3460 cm^{-1} band is now observed with high intensity, which was not observed in the helium-scattering IR spectrum[27] and only appeared with low intensity in the IR-UV spectra of benzene-tagged $(H_2O)_8$[28]. Strikingly, the OH stretch spectra in the 3516–3628 cm^{-1} region include many absorptions spanning multiple vibrational bands, which are considerably more complex than the spectra contributed by high-symmetry D_{2d} and S_4 cubic octamers[27,28], suggesting the presence of more low-symmetry minima of the water octamer.

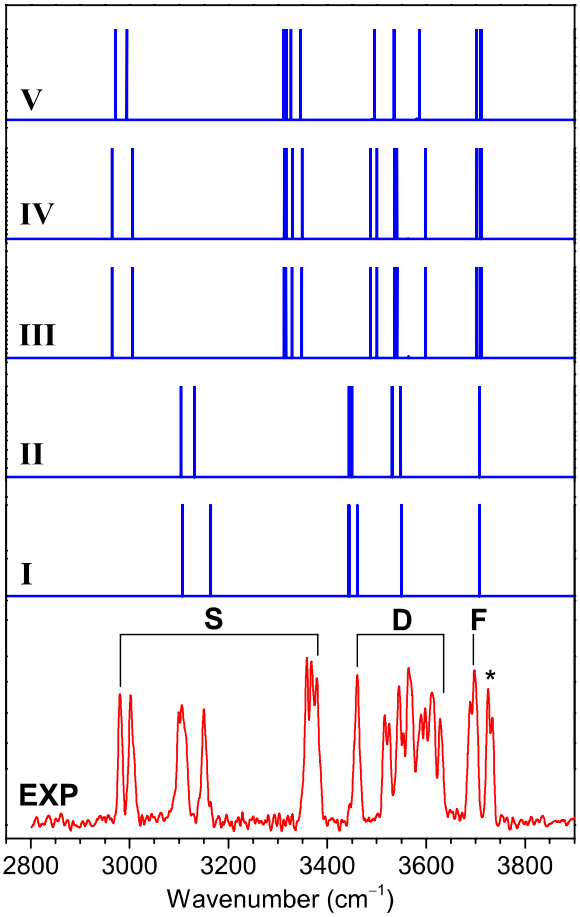

Fig. 1. Comparison of experimental and simulated IR spectra of the water octamer. The OH stretch fundamentals assigned to H-donor-free OH (F), double H-donor OH stretch (D), and single H-donor OH stretch (S) are labeled. The simulated spectra of isomers **I** to **V** are also shown. The calculations were performed at the *ab initio* MP2/aug-cc-pVDZ level, with the harmonic frequencies scaled by 0.956 (See SI for details).

To assign and analyze the observed spectral features, global-minimum structural search based on density functional theory was accomplished for the water octamer using TGMin code[33] (see theoretical details in the SI), which lead to the location of totally 2784 distinct structures. Quantum chemical calculations were carried out to refine the energies of the low-lying isomers (within 11 kcal/mol) (Fig. S2) using *ab initio* MP2/aug-cc-pVDZ (AVDZ) method. The five lowest-energy structures for the water octamer (isomers I–V) are shown in Fig. 2. Each isomer has two classes of hydrogen-bonding environments that we classify as AAD and ADD configurations according to the number of acceptor (A) and donor (D) hydrogen bonds, respectively. The I–V structures differ primarily in the orientation of hydrogen-bonds within the distorted cubes.

As pointed out previously[27,30], direct comparison between theory and experiment for the relative intensities of vibrational bands is very difficult, owing to the complexity of experiment (infrared absorption combined with dissociation, saturation effects) as well as the limitation of theoretical calculation (implicit description of intermolecular zero-point motions). Here, the stick spectra of calculated harmonic vibrational frequencies are utilized to compare with the experimental data. Fig. 1 shows the comparison of experimental spectrum of the water octamer and calculated spectra of isomers I–V. The harmonic OH stretch vibrational frequencies of isomers I–V are listed in Tables S2–S5 and the animation of vibrational modes responsible for the experimental bands is given in the Additional information.

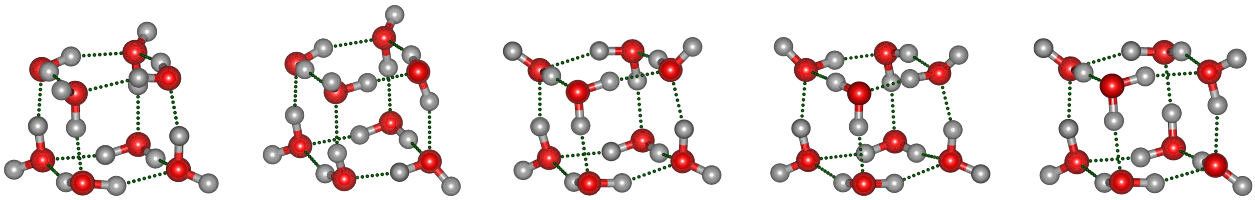

Fig. 2. Optimized structures of coexisting isomers of $(H_2O)_8$. Relative energies from MP2/AVDZ and DLPNO-CCSD(T)/AVTZ (in parenthesis) are listed in kcal/mol.

Each structure of isomers I–V possesses three types of OH groups, namely, the OH of water with single hydrogen-donor configuration (single H-donor OH), double H-donor OH, and H-donor-free OH groups. As noted previously[11,24,27-29], the AAD → ADD hydrogen bonds are remarkably shorter than ADD → AAD hydrogen bonds and the corresponding frequency of single H-donor OH stretch is typically lower than that of double H-donor OH stretch (*vide infra*). Due to the high symmetry of the cubic structures, the normal modes of vibrational stretch of a given type of OH group differ from the other type. As a result, the vibrational frequencies of the single H-donor OH, double H-donor OH, and H-donor-free OH groups are well separated in the OH stretch spectra (Fig. 1 and Tables S2–S5).

In the calculated spectrum of isomer I (D_{2d}) (Fig. 1, trace I), the band positions of single H-donor OH stretches (3107 and 3164 cm^{-1}, Table S2) are consistent with the experimental

values(3106 and 3150 cm^{-1}, Table S1); the calculated transitions at 3443 and 3461 cm^{-1} are attributed to the double H-donor symmetric OH stretches (D^{sym}) and agree with the new experimental absorption centered at 3460 cm^{-1}; the calculated band at 3551 cm^{-1} is due to the double H-donor antisymmetric OH stretches (D^{asym}) and falls in the experimentally spectral range of 3526–3628 cm^{-1}; the calculated H-donor-free OH stretches (3708 cm^{-1}) agree well with the experimental value of 3698 cm^{-1}. The calculated IR spectrum of isomer II (S_4) is rather similar to that of isomer I (D_{2d}) due to analogous geometry. In the isomers I and II, the most significant spectral difference is found in the single H-donor OH stretch region. The two single H-donor OH stretches in isomer II are predicted at 3104 and 3131 cm^{-1} with a separation of 27 cm^{-1} (Table S3), which might be responsible for the broad band observed at 3106 cm^{-1}. The calculated IR spectra of isomers I and II are much too simple to explain the newly observed absorptions at 2980, 3002, and 3378 cm^{-1}, but these features match rather well with those of isomers III, IV, and V (Fig. 1) that are energetically low-lying. Moreover, the III, IV, and V isomers yield various double H-donor OH stretch vibrational fundamentals that cover the spectral range of 3487–3599 cm^{-1} (Tables S4 and S5), which are consistent with the experimentally congested bands in the 3516–3628 cm^{-1} region. The agreement of the calculated spectra with experiment is reasonably good to confirm the assignment of the I–V isomers responsible for the experimental spectra.

In addition, the two well-separated free OH bands at 3698 cm^{-1} (labeled F) and 3726 cm^{-1} (marked with an asterisk) can be related to two distinct AD and AAD sites, because the H-donor free OH groups of the AAD sites generally appear at ~3700 cm^{-1} and those of the AD sites at a higher-frequency range[6,9]. The asterisk-labeled band likely originates from a non-cubic isomer of water-solvated heptamer (Fig. S3). Under the pulsed supersonic expansion condition in the present work, the presence of all five cubic isomers is quite surprising, indicating that our VUV-FEL spectroscopic technique is apt to explore low-lying neutral isomers unknown before.

The five isomers I–V all have interesting cubic structures. The fact that the five cubic isomers I–V lie within 3 kcal/mol indicates that they can possibly coexist according to Boltzmann distribution. The interconversion barrier among them is larger than 4 kcal/mol at the MP2/AVDZ level (Fig. S4). For instance, the interconversion between the two enantiomeric

isomers III and IV need go through four transition states and three intermediates, with the largest barrier of about 5 kcal/mol. Such interconversion barrier might be sufficiently large so that the ultra-high-pressure supersonic expansion cooling is capable of kinetically quenching the nonequilibrium octamer system prior to its rearrangement to the global-minimum energy structure[22]. To evaluate the temperature effect on the distribution of the isomers, Gibbs free energies ΔG of isomers I–V were calculated for the temperature from 0 K to 1000 K (Fig. S5). Clearly, the free energy difference ΔG_{II-I}, ΔG_{III-I}, ΔG_{IV-I}, and ΔG_{V-I} does not alter significantly below room temperature, indicating that the population of the five isomers changes little at low temperature.

To understand the electronic structure of the water octamer, we have analyzed the hydrogen-bond (HB) network of the cubic isomers using delocalized and localized molecular orbital theory. Theoretical approaches were applied of natural bond orbital (NBO)[34], adaptive natural density partitioning (AdNDP)[35], energy decomposition analysis–natural orbitals for chemical valence (EDA-NOCV)[36], and principal interacting orbital (PIO) analysis[37]. Hydrogen bonding between an O-H antibonding orbital (denoted σ*(O–H)) and an adjacent oxygen lone-pair (LP) donor can be viewed as a three-center two-electron (3c-2e) interaction, which features the O lone-pair delocalizing to the H–O antibonding region (Fig. S6)[15,38]. As exemplified by water dimer, the contribution of 3c-2e HB energy to the intrinsic total binding energy (E_{HB}/E_{total}) is about 81.4% from EDA-NOCV analysis, whereas the PIO contribution from the interaction between the lone pair and the σ^*(O–H) antibond is about 88.7% for each 3c-2e HB (Fig. S6). As shown by the bond distances (Tables S7–S11), bond orders, and hybrid orbitals (Table S12), the bond strength of OH groups follows the order of the single H-donor O–H < double H-donor O–H < H-donor-free O–H, which mirrors the extent of electron donation from O lone pair to the $\sigma(OH)^*$ anti-bonding orbitals and accounts for the sequence of the corresponding OH stretch vibrational frequencies observed.

For the water octamer, the E_{HB}/E_{total} values of isomers I–V are all around 89% (Table S6), which are considerably larger than that in the water dimer (81%). This enhanced HB interaction can be partially attributed to the extensively delocalized HB network (*vide infra*). In isomer I (D_{2d}), the AAD → ADD hydrogen bonds (1.698 Å) are much shorter than ADD →

AAD hydrogen bonds (1.904 Å) (Table S7). The NBO second-order perturbation energy (E_2) analysis of the D_{2d} isomer I (Table S7) shows that the AAD → ADD interaction energies (e.g., $E_2(O^1\cdots H\text{-}O^5)$ = 32.17 kcal/mol) are remarkably larger than the ADD → AAD interaction energies (e.g., $E_2(O^1H\cdots O^4)$ = 12.64 kcal/mol), indicating that the face-to-face stacking of the two tetramer rings (O^1-O^2-O^3-O^4 and O^5-O^6-O^7-O^8) is highly favorable. The significantly strong AAD → ADD interactions are also found in the II–V isomers (Tables S8–S11) and benefit the formation of water cubes as well as the stacking of cubic and hexagonal layers that occur in the condensed phase[23,25].

Since the 3c-2e interaction dominates in each HB, we have constructed a secular equation using the Hückel molecular orbital theory. It follows that the 3c-2e HBs are not isolated but highly correlated by delocalized interaction, which leads to extra stabilization when comparing with isolated HBs. This is reminiscent of the aromatic electron delocalization between the single- and double bonds in Kekule structures of benzene. The calculated stabilization energy of delocalized HB network for the D_{2d} isomer I is calculated to be more stable by 4.06 kcal/mol as compared to the isolated HB network (Fig. S7), indicating that the HB network forming an unexpected aromatic delocalization plays a non-negligible role in stabilizing water clusters.

The five water octamer isomers adopting pseudo-cubic structure is highly remarkable. As each O–H···O HB is dominated by the 3c-2e interaction from O lone-pair delocalizing onto the H–O antibonding region, the pseudo-cubic structure can be viewed as consisting of one pair of electron between every two apex oxygen atoms. Interestingly, this bonding pattern is akin to that in the famous cubane (O_h-C_8H_8)[39], where each C–C bond contains two localized electrons, as shown in Fig. 3. While the cubane structure lies much higher in energy than its ring isomer, the D_{2d} cubic isomer of $(H_2O)_8$ lies much lower in energy than the ring isomer, by 11.64 kcal/mol at the *ab initio* DLPNO-CCSD(T)/AVTZ level. Consistent with the extensively delocalized HB interaction, the cubic isomer of water has remarkable thermodynamic stability. ter has remarkable thermodynamic stability.

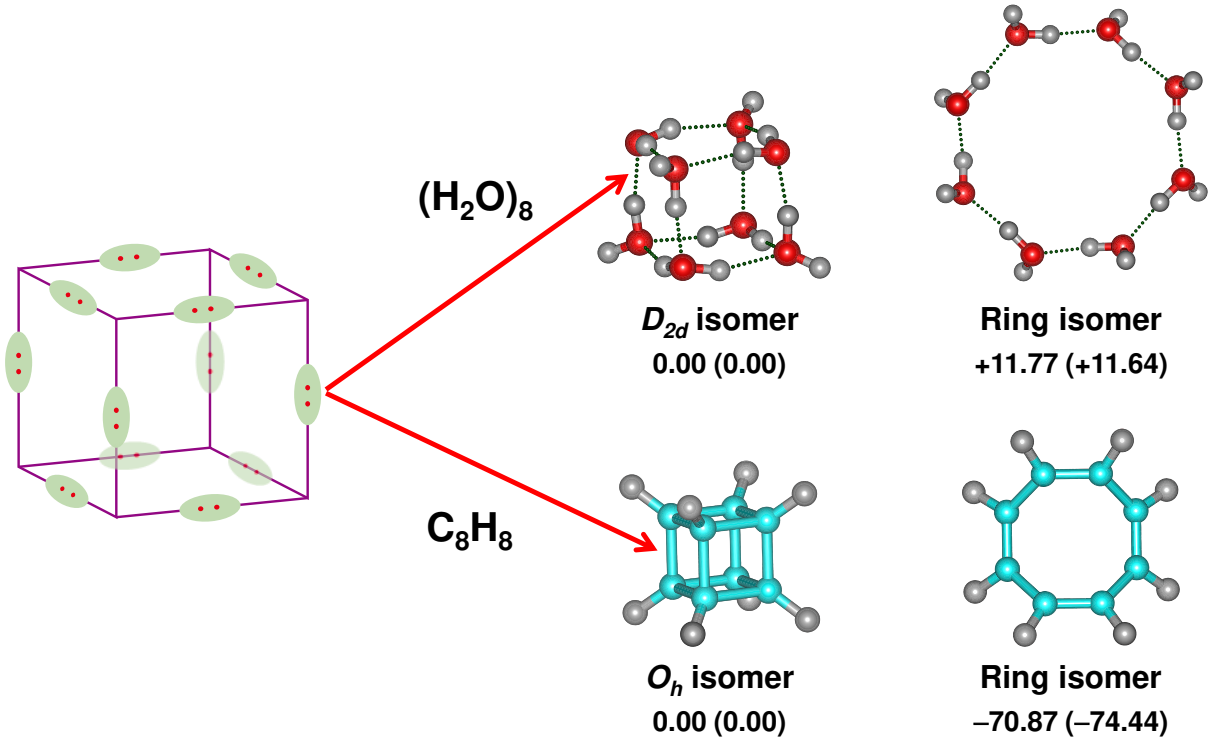

Fig. 3. Analogue of the isomers for $(H_2O)_8$ and C_8H_8. Relative energies from MP2/AVDZ and DLPNO-CCSD(T)/AVTZ (in parenthesis) are listed in kcal/mol.

Especially noteworthy is the finding that the III and IV structures among the five isomers I–V are rare chiral isomers with C_2 symmetry. It is thus interesting to speculate the existence of such transient local chiral structures in bulk water. Previous far-IR vibration-rotation tunneling spectroscopy of chiral cyclic water trimers indicates that rapid quantum tunneling occurs between the enantiomers[10]. Low-temperature scanning tunnelling microscopy shows concerted tunnelling of four protons within chiral cyclic water tetramers supported on an inert surface[40]. The calculated vibrational circular dichroism (VCD) and electronic circular dichroism (ECD) spectra of the two chiral water octamers (isomers III and IV) (Figs. S8 and S9) show clear chiral recognition peaks and provide incentives for future experimental studies.

It is interesting to note that phase transitions between solid and liquid water have been observed in simulations of water clusters as small as the octamer, which is supported by the calculated free energy as a function of temperature[19-22]. The present study has identified the unexpected coexistence of five water octamer cubes that are stabilized by extensive delocalized HB interaction. These findings provide crucial information for understanding the processes of

cloud, aerosol, and ice formation, especially under rapid cooling[41-43]. It is hoped that the present results will both provide a benchmark for accurate description of the water intermolecular potentials to understand the macroscopic properties of water and stimulate further study of intermediate-ice structures formed in the crystallization process of ice.

Data availability

The authors declare that all data supporting the findings of this study are available within the paper and its Supplementary information files.

Acknowledgments

We gratefully acknowledge Mark A. Johnson for helpful discussions. The authors thank the DCLS for VUV-FEL beam time and the DCLS staff for support and assistance. This work was supported by the National Natural Science Foundation of China (21688102, 21673231, 21590792 and 91645203), the Strategic Priority Research Program of Chinese Academy of Sciences (CAS) (XDB17000000), International Partnership Program of CAS (121421KYSB20170012), Dalian Institute of Chemical Physics (DICP DCLS201702), CAS (GJJSTD20190002), the Science Challenge Project (TZ2016004), and Guangdong Key Laboratory of Catalytic Chemistry. The calculations were performed on SUSTech supercomputer.

Author contributions

L.J., J.L., and X.Y. designed the research. G.L., Q.L., C.W., Y.Y., B.Z., W.Z., D.D., G.W., L.J., and X.Y. performed the experiments and data analysis. Y.Y.Z., H.S.H., D.H.Z., and J.L. performed the theoretical calculations and data analysis. L.J., J.L., and X.Y. wrote the manuscript.

Competing interests

The authors declare no competing interests.

Additional information

Supplementary information is available for this paper at the website.

Correspondence and requests for materials should be addressed to L.J., J.L., or X.Y.

References

1. Luzar, A. & Chandler, D. Hydrogen-bond kinetics in liquid water. *Nature* **379**, 55-57 (1996).
2. Mishima, O. & Stanley, H. E. The relationship between liquid, supercooled and glassy water. *Nature* **396**, 329-335 (1998).
3. Liu, K., Cruzan, J. D. & Saykally, R. J. Water clusters. *Science* **271**, 929-933 (1996).
4. Clary, D. C. Quantum dynamics in the smallest water droplet. *Science* **351**, 1267-1268 (2016).
5. Asmis, K. R. *et al.* Gas-phase infrared spectrum of the protonated water dimer. *Science* **299**, 1375-1377 (2003).
6. Miyazaki, M., Fujii, A., Ebata, T. & Mikami, N. Infrared spectroscopic evidence for protonated water clusters forming nanoscale cages. *Science* **304**, 1134-1137 (2004).
7. Shin, J. W. *et al.* Infrared signature of structures associated with the $H^+(H_2O)_n$ (n = 6 to 27) clusters. *Science* **304**, 1137-1140 (2004).
8. Bragg, A. E., Verlet, J. R. R., Kammrath, A., Cheshnovsky, O. & Neumark, D. M. Hydrated electron dynamics: From clusters to bulk. *Science* **306**, 669-671 (2004).
9. Yang, N., Duong, C. H., Kelleher, P. J., McCoy, A. B. & Johnson, M. A. Deconstructing water's diffuse OH stretching vibrational spectrum with cold clusters. *Science* **364**, 275-278 (2019).
10. Pugliano, N. & Saykally, R. J. Measurement of quantum tunneling between chiral isomers of the cyclic water trimer. *Science* **257**, 1937-1940 (1992).
11. Pribble, R. N. & Zwier, T. S. Size-specific infrared spectra of benzene-$(H_2O)_n$ clusters (n = 1 through 7): Evidence for noncyclic $(H_2O)_n$ structures. *Science* **265**, 75-79 (1994).
12. Huisken, F., Kaloudis, M. & Kulcke, A. Infrared spectroscopy of small size-selected water clusters. *J. Chem. Phys.* **104**, 17-25 (1996).
13. Diken, E. G., Robertson, W. H. & Johnson, M. A. The vibrational spectrum of the neutral $(H_2O)_6$ precursor to the "magic" $(H_2O)_6^-$ cluster anion by argon-mediated, population-modulated electron attachment spectroscopy. *J. Phys. Chem. A* **108**, 64-68 (2004).
14. Perez, C. *et al.* Structures of cage, prism, and book isomers of water hexamer from broadband rotational spectroscopy. *Science* **336**, 897-901 (2012).
15. Zhang, B. Infrared spectroscopy of neutral water clusters at finite temperature: Evidence for a noncyclic pentamer. *Proc. Natl. Acad. Sci. USA*, **117**, 15423-15428 (2020).

16. Cruzan, J. D. *et al.* Quantifying hydrogen bond cooperativity in water: VRT spectroscopy of the water tetramer. *Science* **271**, 59-62 (1996).
17. Liu, K., Brown, M. G., Cruzan, J. D. & Saykally, R. J. Vibration-rotation tunneling spectra of the water pentamer: Structure and dynamics. *Science* **271**, 62-64 (1996).
18. Liu, K. *et al.* Characterization of a cage form of the water hexamer. *Nature* **381**, 501-503 (1996).
19. Tsai, C. J. & Jordan, K. D. Use of the histogram and jump-walking methods for overcoming slow barrier crossing behavior in Monte Carlo simulations: Applications to the phase transitions in the Ar_{13} and $(H_2O)_8$ clusters. *J. Chem. Phys.* **99**, 6957-6970 (1993).
20. Laria, D., Rodriguez, J., Dellago, C. & Chandler, D. Dynamical aspects of isomerization and melting transitions in $(H_2O)_8$. *J. Phys. Chem. A* **105**, 2646-2651 (2001).
21. Tharrington, A. N. & Jordan, K. D. Parallel-tempering Monte Carlo study of $(H_2O)_{n=6-9}$. *J. Phys. Chem. A* **107**, 7380-7389 (2003).
22. Jordan, K. D. Smallest water clusters supporting theice I structure. *Proc. Natl. Acad. Sci. USA* **116**, 24383-24385 (2019).
23. Devlin, J. P. Vibrational spectra and point defect activities of icy solids and gas phase clusters. *Int. Rev. Phys. Chem.* **9**, 29-65 (1990).
24. Rowland, B. *et al.* Infrared spectra of ice surfaces and assignment of surface-localized modes from simulated spectra of cubic ice. *J. Chem. Phys.* **102**, 8328-8341 (1995).
25. Buch, V., Bauerecker, S., Devlin, J. P., Buck, U. & Kazimirski, J. K. Solid water clusters in the size range of tens-thousands of H_2O: a combined computational/spectroscopic outlook. *Int. Rev. Phys. Chem.* **23**, 375-433 (2004).
26. Pradzynski, C. C., Forck, R. M., Zeuch, T., Slavicek, P. & Buck, U. A fully size-resolved perspective on the crystallization of water clusters. *Science* **337**, 1529-1532 (2012).
27. Buck, U., Ettischer, I., Melzer, M., Buch, V. & Sadlej, J. Structure and spectra of three-dimensional $(H_2O)_n$ clusters, n = 8, 9, 10. *Phys. Rev. Lett.* **80**, 2578-2581 (1998).
28. Gruenloh, C. J. *et al.* Infrared spectrum of a molecular ice cube: The S_4 and D_{2d} water octamers in benzene-$(water)_8$. *Science* **276**, 1678-1681 (1997).
29. Gruenloh, C. J. *et al.* Resonant ion-dip infrared spectroscopy of the S_4 and D_{2d} wafer octamers in benzene-$(water)_8$ and $benzene_2$-$(water)_8$. *J. Chem. Phys.* **109**, 6601-6614 (1998).
30. Cole, W. T. S., Farrell, J. D., Wales, D. J. & Saykally, R. J. Structure and torsional dynamics of the water octamer from THz laser spectroscopy near 215 μm. *Science* **352**, 1194-1197 (2016).
31. Zhang, B. *et al.* Infrared spectroscopy of neutral water dimer based on a tunable vacuum ultraviolet free electron laser. *J. Phys. Chem. Lett.* **11**, 851-855 (2020).
32. Even, U., Jortner, J., Noy, D., Lavie, N. & Cossart-Magos, C. Cooling of large molecules below 1 K and He clusters formation. *J. Chem. Phys.* **112**, 8068-8071 (2000).

33. Chen, X., Zhao, Y.-F., Wang, L.-S. & Li, J. Recent progresses of global minimum searches of nanoclusters with a constrained Basin-Hopping algorithm in the TGMin program. *Comput. Theor. Chem.* **1107**, 57-65 (2017).
34. Weinhold, F., Landis, C. R. & Glendening, E. D. What is NBO analysis and how is it useful? *Int. Rev. Phys. Chem.* **35**, 399-440 (2016).
35. Zubarev, D. Y. & Boldyrev, A. I. Developing paradigms of chemical bonding: adaptive natural density partitioning. *Phys. Chem. Chem. Phys.* **10**, 5207-5217 (2008).
36. Mitoraj, M. P., Michalak, A. & Ziegler, T. A combined charge and energy decomposition scheme for bond analysis. *J. Chem. Theory Comput.* **5**, 962-975 (2009).
37. Zhang, J.-X., Sheong, F. K. & Lin, Z. Unravelling chemical interactions with principal interacting orbital analysis. *Chem.-Eur. J.* **24**, 9639-9650 (2018).
38. Reed, A. E. & Weinhold, F. Natural bond orbital analysis of near-Hartree-Fock water dimer. *J. Chem. Phys.* **78**, 4066-4073 (1983).
39. Eaton, P. E. & Cole, T. W. Cubane. *J. Am. Chem. Soc.* **86**, 3157-3158 (1964).
40. Meng, X. *et al.* Direct visualization of concerted proton tunnelling in a water nanocluster. *Nature Phys.* **11**, 235-239 (2015).
41. Moore, E. B. & Molinero, V. Structural transformation in supercooled water controls the crystallization rate of ice. *Nature* **479**, 506-508 (2011).
42. Johnston, J. C. & Molinero, V. Crystallization, melting, and structure of water nanoparticles at atmospherically relevant temperatures. *J. Am. Chem. Soc.* **134**, 6650-6659 (2012).
43. Millot, M. *et al.* Nanosecond X-ray diffraction of shock-compressed superionic water ice. *Nature* **569**, 251-255 (2019).

Figures

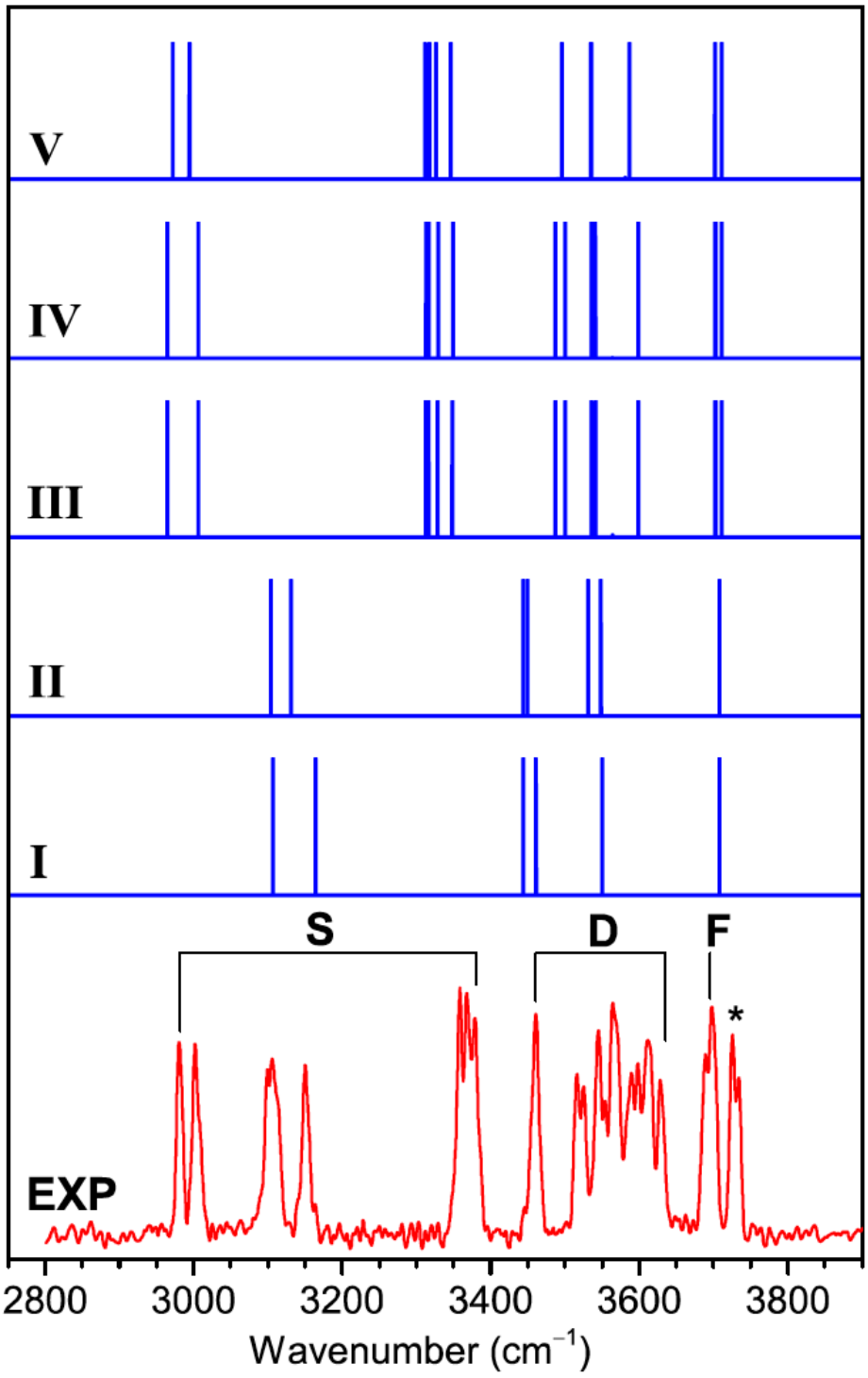

Figure 1

Comparison of experimental and simulated IR spectra of the water octamer. The OH stretch fundamentals assigned to H-donor-free OH (F), double H-donor OH stretch (D), and single H-donor OH stretch (S) are labeled. The simulated spectra of isomers I to V are also shown. The calculations were

performed at the ab initio MP2/aug-cc-pVDZ level, with the harmonic frequencies scaled by 0.956 (See SI for details).

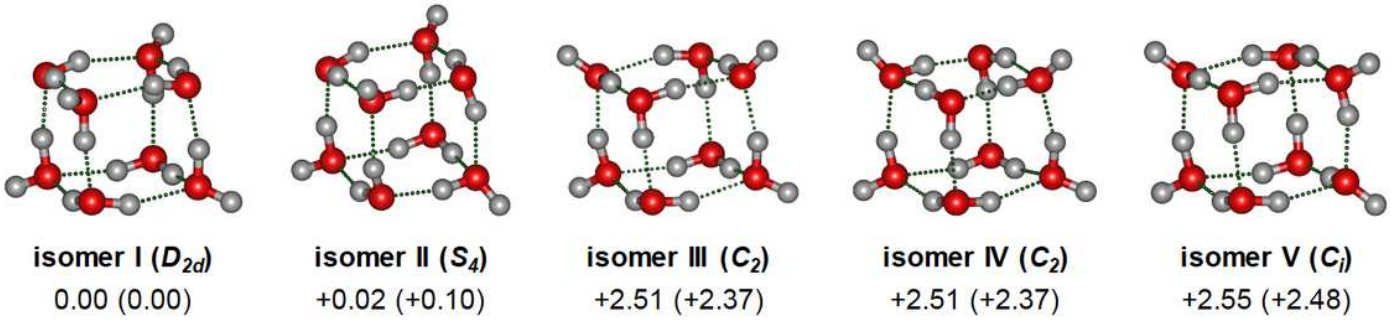

Figure 2

Optimized structures of coexisting isomers of (H2O)8. Relative energies from MP2/AVDZ and DLPNO-CCSD(T)/AVTZ (in parenthesis) are listed in kcal/mol.

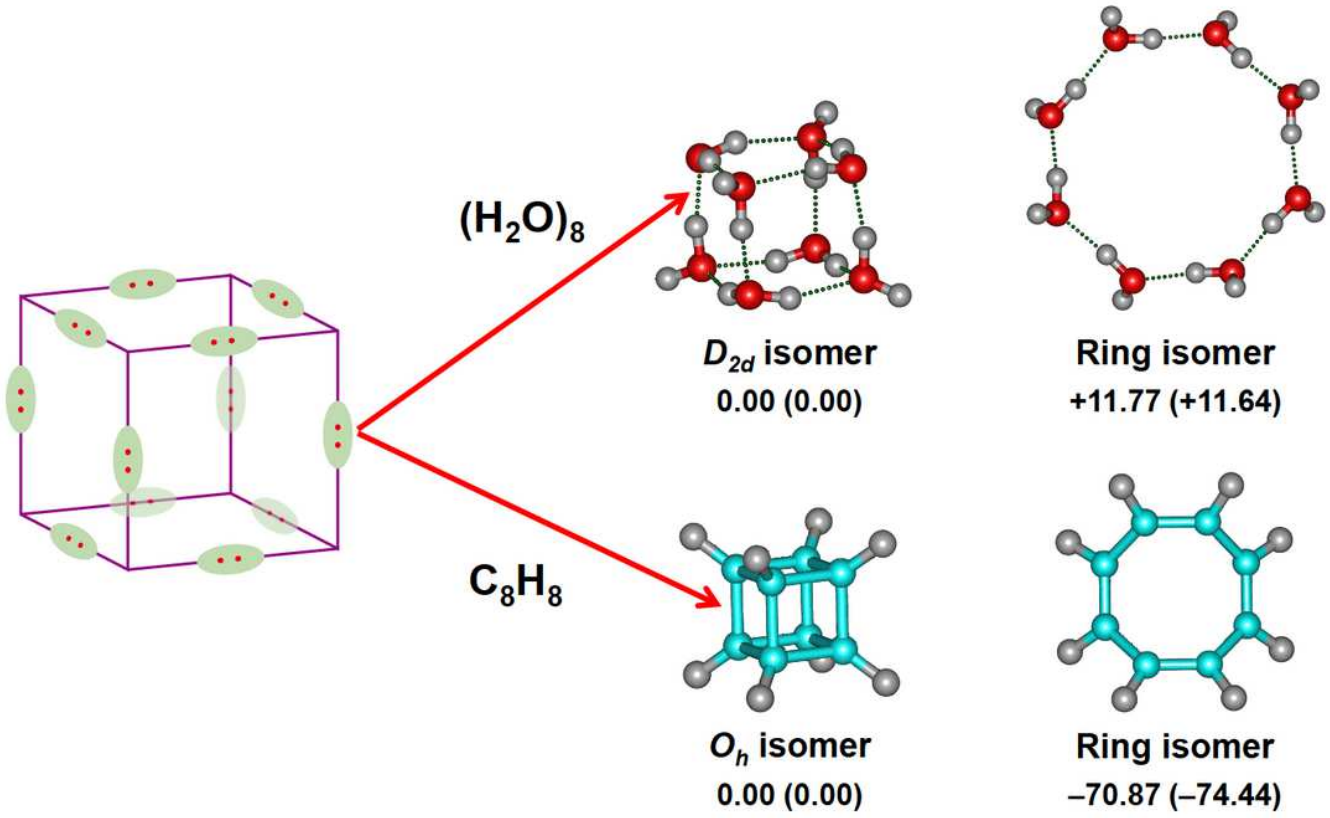

Figure 3

Analogue of the isomers for (H2O)8 and C8H8. Relative energies from MP2/AVDZ and DLPNO-CCSD(T)/AVTZ (in parenthesis) are listed in kcal/mol.

Supplementary Files

This is a list of supplementary files associated with this preprint. Click to download.

- WaterOctamerAnimationofvibrationalmodes20200804.pptx
- WaterOctamerSI20200804.pdf